

40 °C Continuous-Wave Electrically Pumped Hybrid Silicon Evanescent Laser

Hyundai Park^a, Alexander W. Fang^a, Richard Jones^b, Oded Cohen^c, Mario J. Paniccia^b, and John E. Bowers^a

^aUniversity of California Santa Barbara, ECE Department, Santa Barbara, CA 93106, USA

^bIntel Corporation, 2200 Mission College Blvd, SC-12-326, Santa Clara, CA 95054, USA

^cIntel Corporation, SBI Park Har Hotzvim, Jerusalem, 91031, Israel

(to be presented postdeadline at IEEE International Semiconductor Laser Conference Sept. 21, 2006)

Email: hdpark@ece.ucsb.edu

Abstract

We demonstrate an electrically pumped silicon evanescent laser incorporating AlGaInAs quantum wells with a silicon waveguide. The device operates continuous wave with a threshold of 65 mA and a fiber coupled output power of 1.8 mW.

I. Introduction

A room temperature, electrically pumped, silicon laser is one of the last hurdles holding back large scale optical integration onto a silicon photonics platform. Silicon Raman lasers have been demonstrated recently [1, 2], but electrically pumped silicon based lasers have yet to be realized. As an alternative approach, we recently demonstrated an optically-pumped, hybrid silicon evanescent laser [3] as a first step towards electrically pumped laser and other active photonic devices on silicon. In this paper, we report an electrically pumped silicon evanescent laser operating continuous wave at a wavelength of 1.5 μm with a threshold of 65 mA.

II. Device Structure and Fabrication

The silicon evanescent laser is a hybrid device comprised of an offset multiple quantum well region bonded to silicon waveguides that are fabricated on a silicon-on-insulator wafer as shown in Fig.1a. With this architecture, the optical mode can obtain electrically pumped gain from the III-V region while being guided by the underlying silicon waveguide.

The silicon strip waveguide is formed on the (100) surface of an undoped silicon-on-insulator (SOI) substrate with a 2 μm thick buried oxide using standard projection photolithography and $\text{Cl}_2/\text{Ar}/\text{HBr}$ - based plasma reactive ion etching. The silicon waveguide was fabricated with a final height of 0.76 μm and width of 2.5 μm . The epitaxial structure of III-V material grown on InP substrate and its band diagram is shown in Fig. 2 except for 100-nm thick p-InGaAs contact layer doped by 10^{19} cm^{-3} . The multiple quantum well (MQW) region consists of 8 periods of 7-nm thick 1.5Q AlGaInAs wells and 1.3Q AlGaInAs barriers, and is bounded by p-AlGaInAs SCH layer and n-InP and n-InP/InGaAsP superlattice (SL) layers to enable current injection. The SL layer is used to inhibit the propagation of defects from the bonded layer into the quantum well region [4]. The III-V structure is transferred to the patterned silicon wafer via low temperature oxygen plasma assisted wafer bonding [5] described specifically in Ref. 4. After the bonding process, the InP substrate is removed with a mixture of $\text{HCl}/\text{H}_2\text{O}$. 75 μm wide mesas are formed using photolithography and by $\text{CH}_4/\text{H}/\text{Ar}$ -based plasma reactive ion etching through the p-type layers and $\text{H}_3\text{PO}_4/\text{H}_2\text{O}_2$ selective wet etching of the quantum well layers. Ni/AuGe/Ni/Au alloy n-contacts are deposited onto the exposed n-type InP layer and 4 μm wide Pd/Ti/Pd/Au p-contacts are then deposited on the center of the mesas. The p-region on the two sides of the mesa is then implanted with protons for lateral current confinement. The wafer is then diced and the waveguide facets are polished forming an 860 μm long laser cavity. A cross-sectional SEM image of the fabricated device is shown in Fig. 1b. In the fabricated structure, holes are injected through the p-cladding

and the p-SCH layer, and recombine radiatively with electrons injected through thin n-InP and SL layers as shown in Fig. 2. The calculated overlap of the optical mode with the silicon waveguide and the quantum wells is 75 % and 3 % respectively.

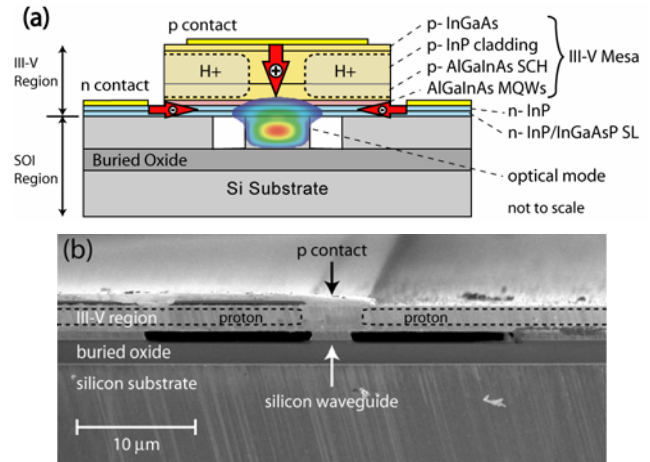


Fig. 1. (a) Cross sectional device structure. (b) SEM image

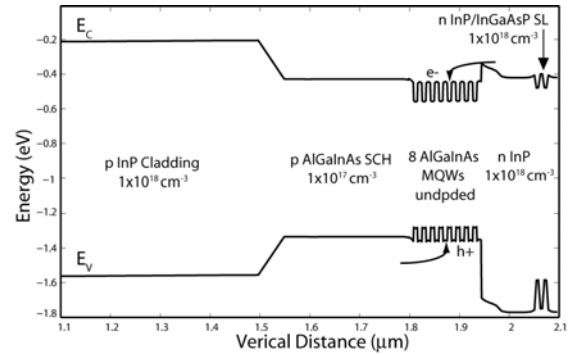


Fig. 2. Band structure of epitaxial layers.

III. Experimental Result

The laser is driven by applying a positive bias voltage to the top p contact. Figure 3 shows LI curve for various operating temperatures ranging from 15 to 40 °C. The threshold is 65 mA with a maximum fiber coupled output power of 1.8 mW at 15 °C. The differential quantum efficiency is estimated to be 12.7 % taking account the measured 6 dB coupling loss from waveguide to fiber, and the fact that light is only collected from one facet. The maximum c.w. operating temperature is 40 °C and the characteristic temperature (T_0) is measured to be 39 K. In addition, the lasers showed pulsed lasing up to 80 °C even without proton implantation under pulsed current excitation. The laser has a threshold voltage of 2 V and a series resistance of 7.5 ohms as shown in the dotted line of Fig. 3b.

Most of the series resistance is attributed to the thin n type layers whose sheet resistance is measured to be 200 ohm/ \square by TLMs.

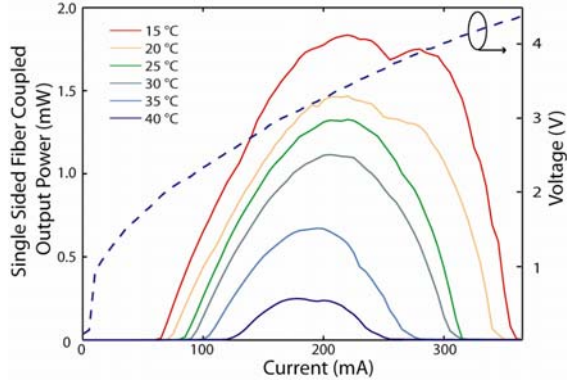


Fig. 3. c.w. LI curves. (dotted) IV curve.

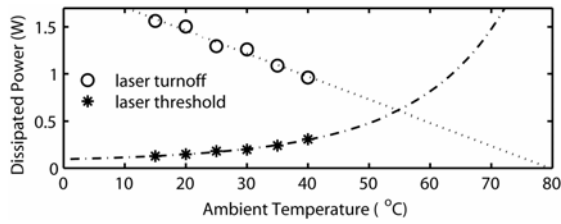


Fig. 4. Dissipated electrical power at the threshold and laser turnoff.

Figure 4 shows the dissipated electrical power at laser threshold and laser turn off. The thermal resistance of 40 °C/W is extracted from the slope of the dissipated power at the laser turnoff. In addition, the x-intercept of 80 °C of the line is the maximum temperature for lasing, which is ideally the maximum temperature of pulsed operation [6]. Narrowing the distance between the n-contact and the center of the waveguide from 38 μm down to less than 10 μm can reduce the series resistance down to ~ 2 ohms improving the temperature performance significantly. Moreover, simulation shows that the buried oxide thickness reduction from 2 μm to 1 μm will reduce the thermal resistance from 40 °C/W to 28 °C/W leading to better heat extraction from the active region. In addition to reduction of electrical and thermal resistance, lasing threshold reduction would also improve the temperature performance. Figure 5 shows the predicted thresholds calculated from a measured modal loss of 15 cm^{-1} and an injection efficiency of 70 %. Sub 10 mA threshold should be achievable with high reflection coating of ~ 90 %.

Improvements to current confinement such as optimization of the proton implantation profile should improve injection efficiency up to 90 % to further reduce the threshold.

Figure 6 shows the lasing spectra at three different currents. The lasing wavelength is around 1577 nm near the threshold and is shifted to longer wavelengths as the current increases due to device heating. The Fabry-Perot fringe spacing of 0.38 nm corresponds to a group index of 3.68.

channels provide lower threshold because of increased lateral carrier confinement. Other bars made with the same bond step showed similar or better yields. The yield should be greatly improved by utilizing integrated laser cavity feedback techniques, such as ring resonators or gratings to avoid waveguide chipping and bond delamination caused by polishing.

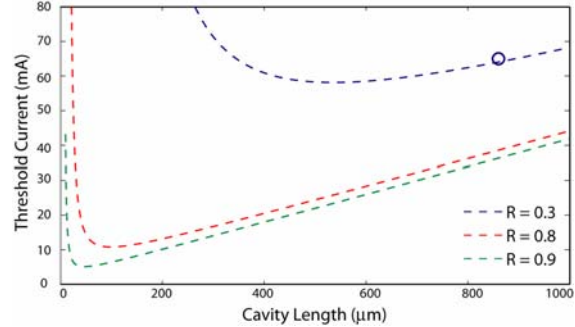


Fig. 5. Calculated threshold vs cavity length with different facet reflectivity.

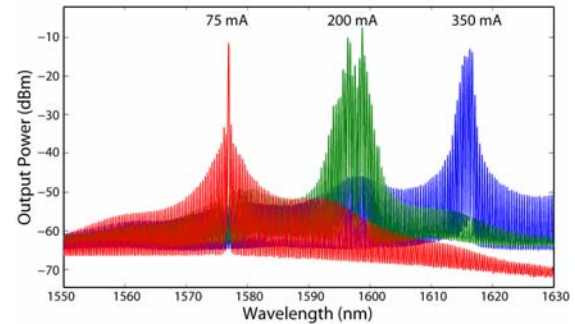


Fig. 6. Lasing spectra with three different current levels.

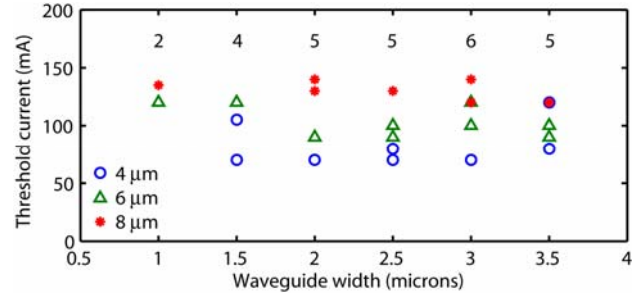


Fig. 7. Threshold variation with different waveguide widths.

IV. Conclusion

We have demonstrated a c.w. electrically pumped hybrid silicon evanescent laser with 65 mA threshold, 1.8 mW output power and differential quantum efficiency of 12.7 % that lases c.w. up to 40 °C. This research is an important step towards the realization of cost-effective, highly integrated silicon photonic devices.

References

- [1] H. Rong, *et al.*, *Nature* **433**, 725, (2005).
- [2] O. Boyraz, *et al.*, *Opt. Express* **12**, 5269, (2004).
- [3] H. Park, *et al.*, *Opt. Express* **13**, 9460 (2005).
- [4] A. Karim, *et al.*, *PTL* **12**, 1438, (2000).
- [5] D. Pasquariello, *et al.*, *JSTQE* **8**, 118, (2002).
- [6] N. Margalit, Ph.D. Thesis, UCSB, (1998).

Acknowledgement

This work was supported by DARPA through contracts W911NF-05-1-0175 and W911NF-04-9-0001, and by Intel. The authors thank Jag Shah and Wayne Chang for useful discussions.